ARL-TR-7620 ● MAR 2016

US Army Research Laboratory

Characterization of Novel Gel-Casting System to Make Complex-Shaped Aluminum Oxide (Al_2O_3) Parts

by Carli A Moorehead, Victoria L Blair, and Jane W Adams

NOTICES

Disclaimers

The findings in this report are not to be construed as an official Department of the Army position unless so designated by other authorized documents.

Citation of manufacturer's or trade names does not constitute an official endorsement or approval of the use thereof.

Destroy this report when it is no longer needed. Do not return it to the originator.

ARL-TR-7620 ● MAR 2016

US Army Research Laboratory

Characterization of Novel Gel-Casting System to Make Complex-Shaped Aluminum Oxide (Al_2O_3) Parts

by Carli A Moorehead
Drexel University

Victoria L Blair and Jane W Adams
Weapons and Materials Research Directorate, ARL

REPORT DOCUMENTATION PAGE

Form Approved
OMB No. 0704-0188

1. REPORT DATE *(DD-MM-YYYY)*	2. REPORT TYPE	3. DATES COVERED (From - To)
March 2016	Final	March 2015–December 2015

4. TITLE AND SUBTITLE
Characterization of Novel Gel-Casting System to Make Complex-Shaped Aluminum Oxide (Al_2O_3) Parts

5a. CONTRACT NUMBER

5b. GRANT NUMBER

5c. PROGRAM ELEMENT NUMBER

6. AUTHOR(S)
Carli A Moorehead, Victoria L Blair, and Jane W Adams

5d. PROJECT NUMBER
DSI14-WM-014

5e. TASK NUMBER

5f. WORK UNIT NUMBER

7. PERFORMING ORGANIZATION NAME(S) AND ADDRESS(ES)
US Army Research Laboratory
ATTN: RDRL-WMM-E
Aberdeen Proving Ground, MD 21005-5069

8. PERFORMING ORGANIZATION REPORT NUMBER
ARL-TR-7620

9. SPONSORING/MONITORING AGENCY NAME(S) AND ADDRESS(ES)

10. SPONSOR/MONITOR'S ACRONYM(S)

11. SPONSOR/MONITOR'S REPORT NUMBER(S)

12. DISTRIBUTION/AVAILABILITY STATEMENT
Approved for public release; distribution is unlimited.

13. SUPPLEMENTARY NOTES

14. ABSTRACT
This work describes the characterization of a novel gel-casting system using a water-soluble co-polymer of isobutylene and maleic anhydride (trade name ISOBAM). This system enables ceramic slurries to gel at very low binder concentrations (0.3–0.5 wt%), producing a dense, near-net-shaped green body with high solids loading, low organic content, low shrinkage, and moderate strength. The effect of both binder content and solids loading on gel time and mechanical strength of green bodies is investigated along with typical shrinkage and densification rates of both green and sintered parts. Additionally, the effect of primary particle size and surface area on slurry and gelling behavior is explored to determine if a relationship exists that can help predict appropriate slurry formula parameters.

15. SUBJECT TERMS
gel-casting, ISOBAM, characterization, mechanical strength, water-soluble gelling system

16. SECURITY CLASSIFICATION OF:			17. LIMITATION OF ABSTRACT	18. NUMBER OF PAGES	19a. NAME OF RESPONSIBLE PERSON
a. REPORT	b. ABSTRACT	c. THIS PAGE			Victoria L Blair
Unclassified	Unclassified	Unclassified	UU	26	19b. TELEPHONE NUMBER (Include area code) 410-306-4947

Contents

List of Figures

List of Tables

Acknowledgments

Special thanks to Dr Nicholas Ku for assistance with powder characterization and Drs Joshua Orlicki and Anit Giri for their assistance with the differential scanning calorimetry and thermal gravimetric analysis and mass spectroscopy measurements.

INTENTIONALLY LEFT BLANK.

1. Introduction

Since its invention during the 1990s, gel-casting has been an attractive technique for producing dense, near-net-shaped ceramic parts, as casting mitigates often costly and wasteful machining steps.[1] However, since it is a relatively new technique, it has many inherent issues that have limited its usefulness. Typically, several polymeric components (monomer, dispersant, cross-linker, and activator) are used to create an in situ network around the dispersed ceramic particles to hold them in place while they are sintered to ensure a dense microstructure free of pores.[1–10] Traditional systems include acrylics, cellulose ethers, and polyvinyl alcohols[11,12]; however, some natural organic polymer systems have been investigated including systems based on starch, gelatin, protein, and agarose. Generally, all systems are too expensive for high-volume casting.[13] While gel-casting has been used frequently to produce thin coatings and tapes, larger cast bodies often develop cracks because of the high-capillary stresses produced during drying.[1,10] Other issues may arise from 1) low solids loading, which leads to high shrinkage rates and/or uneven shrinkage and cracking; 2) costly, often toxic organic components; and 3) cracking and warping during a time-consuming binder burn-out (due to the high volume of organic phase that must be removed and occasionally produces a large volume of toxic exhaust depending on the binder choice).[1,3,5,6,8,9]

Recently, a novel, self-assembling gel-casting system using a water-soluble alternating co-polymer of isobutylene and maleic anhydride (Fig. 1) with the trade name ISOBAM has gained interest. It is particularly advantageous because it uses one organic component that acts as both a binder and dispersant at very low concentrations but produces dense green bodies with homogenous microstructures at high solids loading (up to 81 vol%),[3] low added organic content (<1 wt% with respect to the ceramic powder component),[2–4,6,8–10,12–17] low shrinkage, and no cracking.[2–6,8–17] While the gelling mechanism is unknown, it is theorized to be based on surface interactions between ceramic particles and the long chains of polymer that wrap around the particles and interact with each other, creating an elastomer network of intramolecular interactions.[4,5,8,14] The ISOBAM system has been used to produce a range of bulk ceramic parts including both dense [6,8–11,17] and porous[16] alumina, porous silicon nitride,[2,13] both porous[12] and dense[5] mullite, dense AlN (aluminum nitride),[4] dense AlON (aluminum oxynitride),[15] transparent Y_2O_3 (yttrium oxide),[3] and transparent YAG (yttrium aluminum garnet).[14]

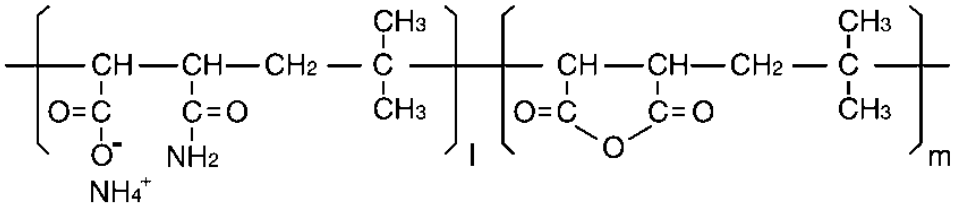

Fig. 1 Molecular structure of the ISOBAM polymer, where *l* and *m* represent the 2 types of monomer that alternate linearly along the chain

Previous work has attempted to characterize the gelling system by extensively investigating the effect of both solids loading and binder content on viscosity,[2–4,8–12,14] storage modulus,[3,4,8–10,12] and zeta potential.[4,8–10,12,14] Work has also been done to characterize shrinkage[10] and densification[6] rates for this system, although more work is needed in these areas. Additionally, no work had been specifically conducted to determine the effect of process variables on the mechanical strength of cast green bodies or the effect of particle size and particle surface area changes on the gelling behavior and slurry parameters. This work aims to fill the gaps in the literature and more robustly characterize the ISOBAM gel-casting system so that it is better understood and can be tailored to specific applications.

This report describes the analysis of the effect of both binder content and solids loading on gel time and modulus of rupture in green bodies, in addition to characterizing typical shrinkage and density rates in the context of commercially available alumina. It also describes the adaptation of the ISOBAM gelling system to different-sized alumina particles and the possible relationship between particle surface area and slurry water content (solids loading) to achieve reasonable casting behavior.

2. Methods and Materials

2.1 Materials

Commercial samples of a co-polymer (1:1) of isobutylene and maleic anhydride (trade name ISOBAM) were obtained from Kuraray (Kuraray America, Elastomer BU, Houston, TX). ISOBAM #110 and ISOBAM #104 were used. Both grades were of the amide-ammonium type, which readily dissolve in water. The #104 grade had an average molecular weight of 55–65 kDa while the #110 grade had an average molecular weight of 160–170 kDa.

Four alumina powders produced by the Bayer processing technique were acquired from Almatis (Almatis Inc., Leetsdale, PA) and Alcoa (Alcoa Global, New York, NY). Alcoa A14-325, Alcoa A16, Almatis A3500-UG, and Almatis A16-SG were used. Additionally, the Alcoa A16 powder was ball milled to reduce the hard agglomerates and provide a sixth powder for examination.

Nano-sized alumina powder was obtained via a co-precipitation method. High-purity nitrates of aluminum, erbium (to enhance properties for intended application as a laser host media), and magnesium (sintering aid, 250 ppm) were dissolved in water and added drop-wise with a basic solution of ammonium bicarbonate and ammonium hydroxide into a buffer solution of ammonium bicarbonate. This resulted in an aluminum-ammonium-carbonate-hydrate that converted to $Er_{0.002}Al_{1.998}O_3$ upon calcination. The resulting precipitate was washed 3 times to remove excess salts and then dried in an oven at approximately 60 °C. The synthesized powder was calcined at 1,300 °C for 30 min (10 °C/min heating and cooling rate) to ensure pure α-Al_2O_3 (alpha aluminum oxide) composition.

Each of the 6 alumina samples was characterized using low-temperature nitrogen-absorption BET (Micromeritics ASAP 2010) to establish particle surface area and laser anemometry to determine particle size distribution. Tap density was also performed to calculate the volume loading of the slurries using a 10-mL graduated cylinder to approximate the volume of a known mass of powder.

In an effort to gain more understanding into formulation of the gel-casting process, different alumina powders with different particle sizes and surface areas were gel-cast into parts. All 6 alumina powder samples (5 synthesized by Bayer process and one by chemical precipitation process) were used to load slurries until the maximum solids load was reached at a constant binder content of 0.3 solids wt%. The resulting solids loading values (in vol% and wt%) at maximum solids loading were analyzed to determine if any trends could be detected based on either the powder particle surface area or average primary particle size.

2.2 Gel-Casting Procedure

Recipes for gel-casting were calculated by weight-percent. Also, the amount of ISOBAM to be added was calculated on the basis of total solids. For example, the amount of binder added would be 0.3 wt% of the total solids added to the process. The calculated portions of deionized water and ISOBAM were added to a small beaker over a magnetic stir plate to dissolve the ISOBAM. Once dissolved, the appropriate amount of alumina was added while gradually increasing the speed of the stir bar as the mixture became more viscous. The slurry was allowed to mix for 30 min before casting into a lubricated, polyurethane (PU) mold. The mold was

previously coated with a thin film of WD-40 (WD-40 Co., San Diego, CA) to prevent wall interaction stress that could lead to cracks in the green body as it gelled and dried. After casting, the green body was allowed to set at room temperature on the bench-top for approximately 16 h. The part was then demolded by inverting the mold and dried in a 60 °C oven for approximately 48 h to drive off residual moisture.

2.3 Gel Time Determination

Determination of the optimal gelation times was assessed by varying the solids loading and binder content. Sample sets consisted of solids loading from 60 to 75 wt% while keeping binder content constant at 0.3 powder wt% and varying binder content from 0.1 to 0.7 solids wt% while keeping solids loading constant at 70 wt%. The specimen was considered "gelled" by observing the cessation of flow in the casting. The cessation of flow was determined by measuring the resistance force in uniaxial compression. Therefore, the specimen was considered gelled when the resistance force was greater than 0.5 N, as the slurries would no longer have an observable flow at that force. A broad indentation tip was machined with the dimensions of the tip displayed in Fig. 2. The tip was slightly beveled to remove sharp corners and reduce possible surface tension issues among the varied samples.

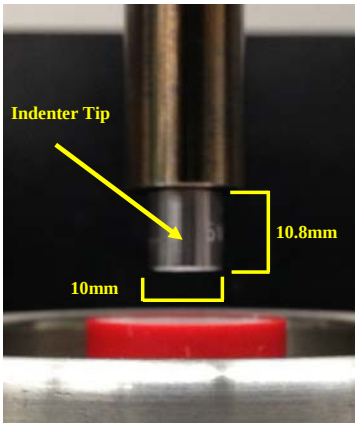

Fig. 2 Custom indenter tip machined for gel time testing with dimensions marked (dimensions do not include the bevel)

The beveled indenter was attached to a Zwick Z030 load frame (Zwick USA, Kennesaw, GA), which measured the uniaxial load to estimate gel-time. The testing software was used to lower the indenter tip at a rate of 30 mm/min by a distance of 6 mm while measuring the maximum resistance force during the indentation. At the start of each test, the indenter tip was lined up with the surface of the slurry to keep the starting position relative to the cast roughly equal. For each test, a set of

8–12 samples from a single batch of slurry were cast in 1-inch cylindrical plastic potting molds. Specimens were evaluated at increasing time intervals with respect to how long it took each composition to set.

2.4 Green Body Mechanical Testing

Mechanical testing was carried out to determine the effects of process variables such as solids loading and binder content on the strength of cast green bodies. Samples of the following compositions (Table 1) were cast into approximately 2- × 2-inches PU mold coated with WD-40. After setting approximately 16 h, demolding, and drying (~60 °C for ~48 h), samples were cut on diamond-impregnated wire saw (Model 850, South Bay Technologies, San Clemente, CA) into bend bards approximately 43 x 6 x 8 mm in size. The dimensions for each sample were measured individually before testing and used to calculate modulus of rupture using Eq. 1,

$$MOR = \frac{3FL}{2bh^2}, \tag{1}$$

where F denotes force at failure (maximum force), L is the distance between support fixtures (40 mm in this case), b denotes the width of the sample, and h is the height of the sample.

Table 1 Design matrix for mechanical testing

Solids loading (wt%)	No. of specimens Solids weight percent ISOBAM		
	0.1 wt%	0.3 wt%	0.7 wt%
70	31	25	18
73	. . .	22	. . .
75	. . .	15	. . .

Samples were tested using an ASTM 40- × 3- × 4-mm 3-point bend testing fixture on a load frame (Model 5500R1123, Instron, Norwood, MA) equipped with a 1-kN compression load cell. Testing was conducted at a rate of 0.500 mm/min. The force at failure was recorded and used to calculate the modulus of rupture to account for differences in sample geometry. For each series, binder content and solids loading variations were assessed using one-way analysis of variance followed by Tukey's HSD test to detect significant differences in strength.

2.5 Shrinkage and Density Measurements

Specimens were generated by gel-casting Alcoa A16 powder with 73 wt% solids loading and 0.3 solids wt% binder content. The density measurements were performed on pre-sintered bodies via geometric measurements (as green bodies will

dissolve in water) and on sintered bodies using Archimedes principle (AX205 DeltaRange, Mettler Toledo, Columbus, OH). Density was calculated as a percentage of theoretical density by normalizing to the theoretical density of α-Al_2O_3, which is widely accepted as approximately 3.94 g/cm^2. Three specimens were generated and analyzed out of each process step. Each dimension was recorded 5 times and the results averaged to minimize measurement errors.

Measurements for linear and volume shrinkage of bodies were taken at each stage of processing including as-cast (based on the mold interior size), demolded after a 16-h room temperature drying period, oven dried after a 48-h drying period in a 60 °C oven, and sintered. Sintering was carried out in an alumina boat at heating/hold/cooling rates as shown in Fig. 3. Percentage shrinkage was calculated by normalizing to the original cast dimensions.

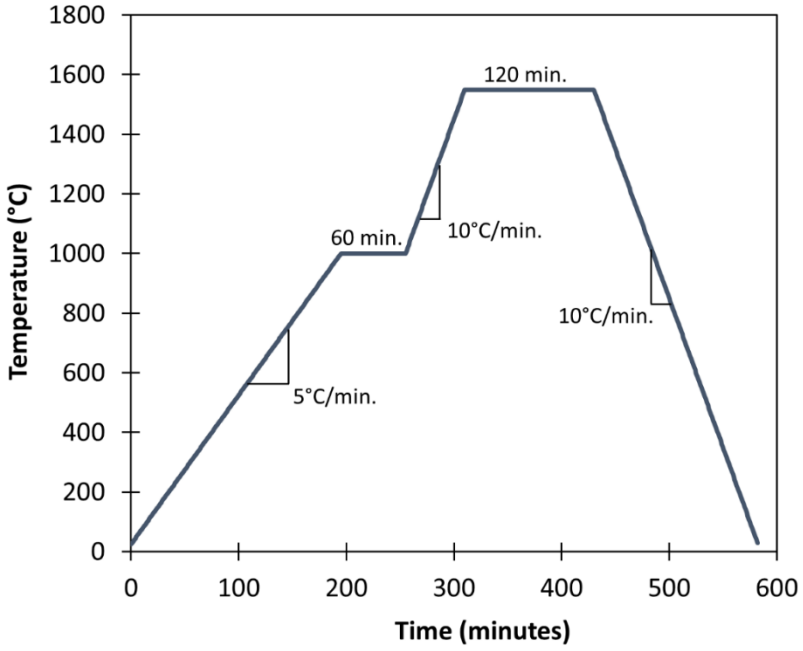

Fig. 3 Furnace cycle schedule for the sintered gel-cast specimens used for shrinkage and density measurements

3. Results

3.1 Determination of Gelation Time

Figure 4 shows the gel time curves for different solids loadings, while Fig. 5 shows the curves for different binder content. Using approximately 0.5 N as the force at initial gelling, Tables 2 and 3 list the initial gel times for the solids loading and binder content series, respectively.

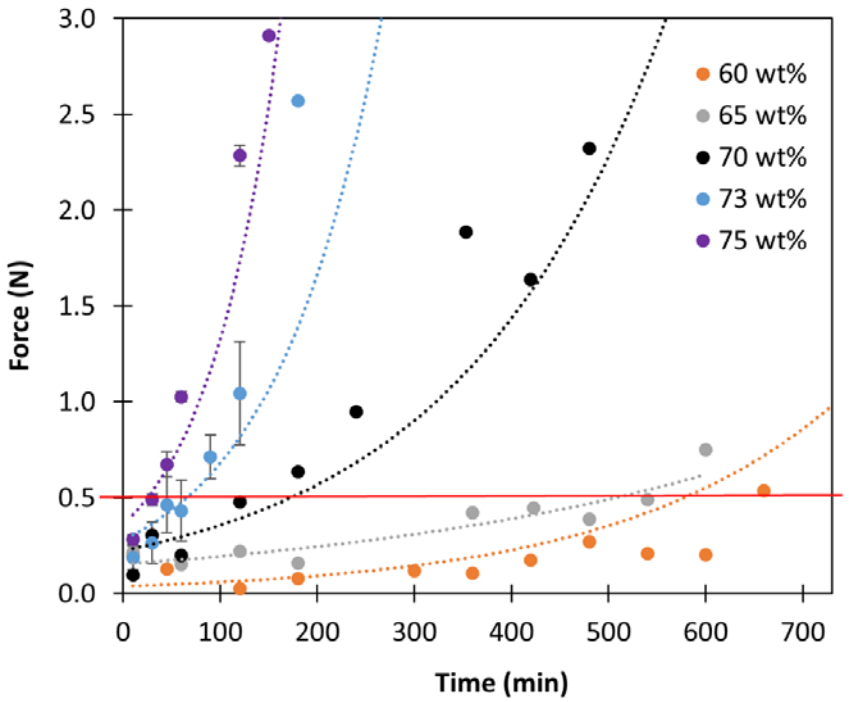

Fig. 4 Set time curves with varying solids loading at 0.3 wt% binder. The red line represents the force at which the samples have gelled. Data points with error bars indicate N = 3.

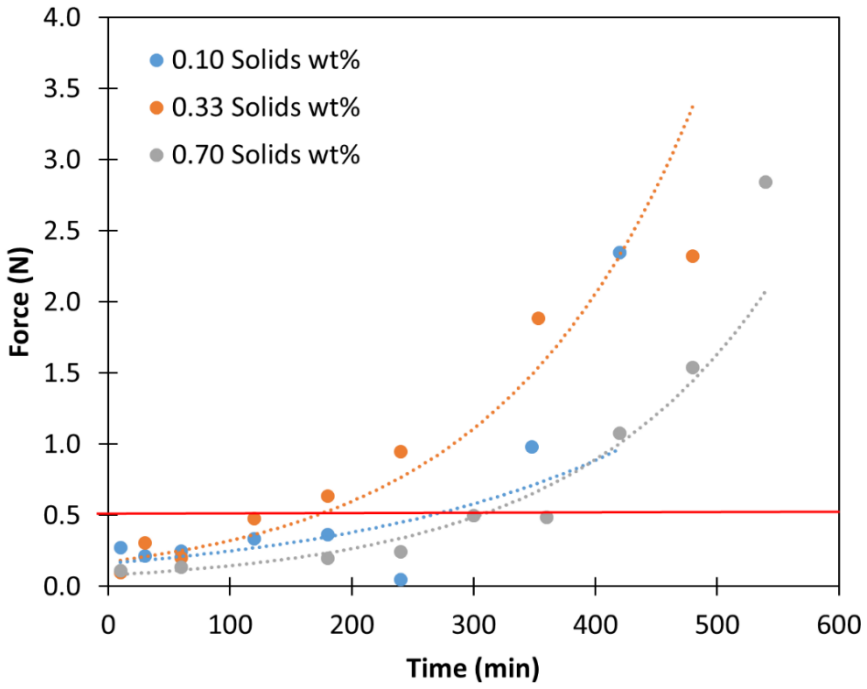

Fig. 5 Set time curves with varying binder content. The red line represents the force at which the samples have gelled.

Table 2 Set time changes with solids loading

Solids loading (wt%)	Setting time (h)
60.0	11.0
65.0	9.0
70.0	2.0
73.2	0.8
75.0	0.5

Table 3 Set time changes with binder content

Binder content (wt%)	Setting time (h)
0.10	5
0.33	2
0.70	6

It is clear from Table 2 and Fig. 4 that gel time is highly influenced by the solids loading of the slurry. Gel times ranged from 30 min to 11 h when solids loading varied from 60 to 75 wt%. It was determined that the most influential factor when trying to modulate the gel time of a slurry was the solids loading, with an ideal viscosity and set time for typical gel-casting applications occurring at approximately 73% for approximately 0.5-μm alumina. Gel time was also affected by the binder content. The technical information supplied by Kuraray showed that at 0.3 solids wt% ISOBAM, a minimum viscosity was achieved.

3.2 Shrinkage and Density Measurements

The average linear dimension shrinkage, volume percent change, and density as a percentage of theoretical density (TD) are listed in Table 4. All shrinkages decreased initially at demolding, increased slightly after drying, and decreased substantially upon sintering (Fig. 6). The density followed a similar trend, increasing initially (higher density), decreasing after drying, and increasing substantially upon sintering.

Table 4 Shrinkage and density changes throughout processing sequence. Results are reported in average ± standard deviation between samples (N = 3).

Stage	Diameter shrinkage (%)	Thickness shrinkage (%)	Volume shrinkage (%)	Density (% TD)
As cast	0.00 ± 0.00	0.00 ± 0.00	0.00 ± 0.00	58.4 ± 0.20
demolded	4.23 ± 0.83	7.66 ± 1.61	15.3 ± 2.6	60.7 ± 1.1
dried	3.72 ± 0.64	6.49 ± 2.28	13.3 ± 1.3	49.5 ± 0.9
sintered	21.7 ± 0.8	23.1 ± 1.5	52.8 ± 1.2	97.4 ± 0.6

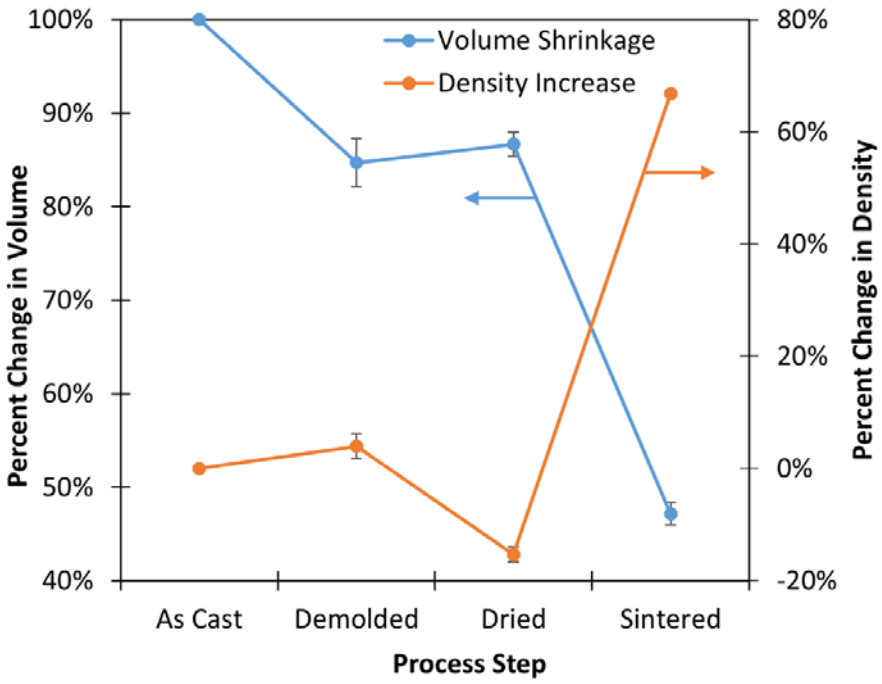

Fig. 6 Density and volume changes throughout the processing sequence. Shrinkage is reported as a percentage of original volume (as-cast) and densities are reported as a percentage increase over the as-cast part.

The cast experienced slight shrinkage during the green body phase and substantial shrinkage during sintering, which is common with gel-casting techniques. The density increased as the slurry settled into the mold, decreased as the excess water was dried out of the green body and capillary stress was removed, and increased substantially during sintering.

3.3 Mechanical Strength of Green Bodies

Figure 7 shows strength increases with both solids loading and binder content, with Tables 5 and 6 showing the plotted data. This was confirmed when 1–3 solids wt% gel-cast specimens were cast and ground. While standard samples (0.3 solids wt% binder) could be crushed using a mortar and pestle, the higher binder content samples were very hard and had to be crushed using a hammer mill. This was expected since increasing the binder in gel-casting generally increases the strength of the network holding the particles in place.

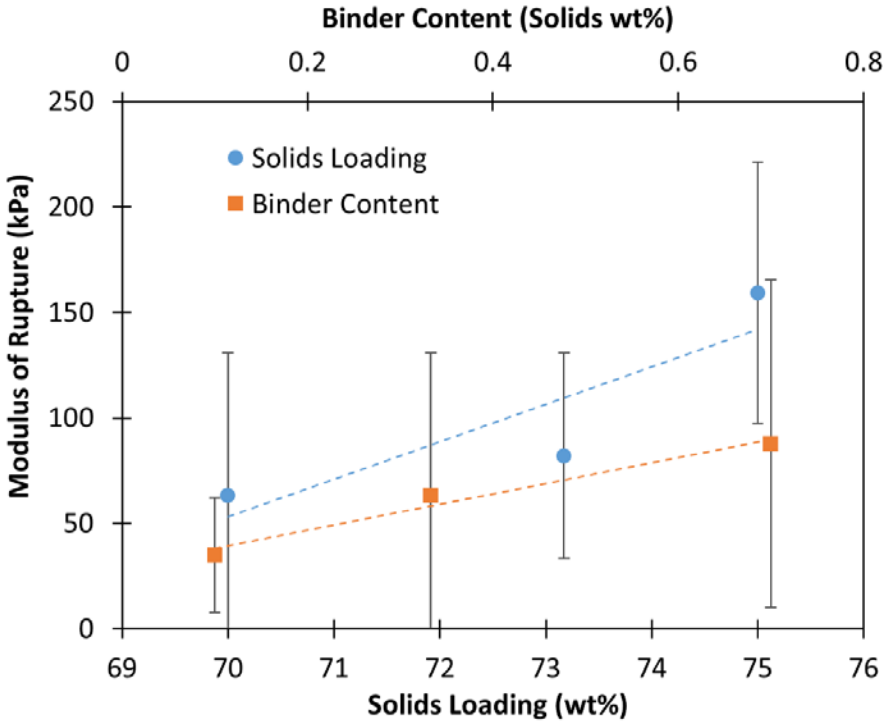

Fig. 7 Green body strength trends with changes in solids loading a binder content

Table 5 Three-point bend testing results varying solids loading. Values are reported in average ± standard deviation.

Solids loading effects	
Solids loading (wt%)	**Average failure stress (kPa)**
70	63.1 ± 67.7[a+]
73.2	82.0 ± 48.7[a]
75	159.3 ± 62.1[+]

[a] Indicates one pair that was found to be significantly different ($p<0.05$), [+] indicates another.

Table 6 Three-point bend testing results varying binder content. Values are reported in average ± standard deviation.

Binder content effects	
Binder content (wt%)	**Average failure stress (kPa)**
0.1 solids	35.0 ± 27.1[a]
0.33 solids	63.1 ± 67.7
0.7 solids	87.8 ± 77.5 [a]

[a] Significantly different ($p<0.05$).

3.4 Slurry Behavior Trends with Surface Area and Particle Size

The results of both particle surface area and particle surface distribution characterization of the 6 alumina samples used are shown in Table 7 along with the volume-percent and weight-percent solids loading (for slurries of optimal gelling behavior and viscosity). Solids loading by weight-percent and volume-percent were plotted against particle size and particle surface area. The results are displayed in Fig. 8.

Table 7 Powder characterization results and optimal solids loading (vol% and wt%) for each powder sample

Powder sample	Surface area (m^2/g)	Average primary particle size (µm)	Solids loading (vol%)	Solids loading (wt%)
Alcoa A16	7.67	0.67	68	73
Ball milled alcoa A16	8.62	0.39	66	70
Alcoa A14-325	0.32	8.25	70	76
Almatis A16-SG	6.85	0.78	64	73
Almatis A3500-UG	2.87	3.50	73	82
Er:Al_2O_3 via precipitation process	26.48	0.31	68	45

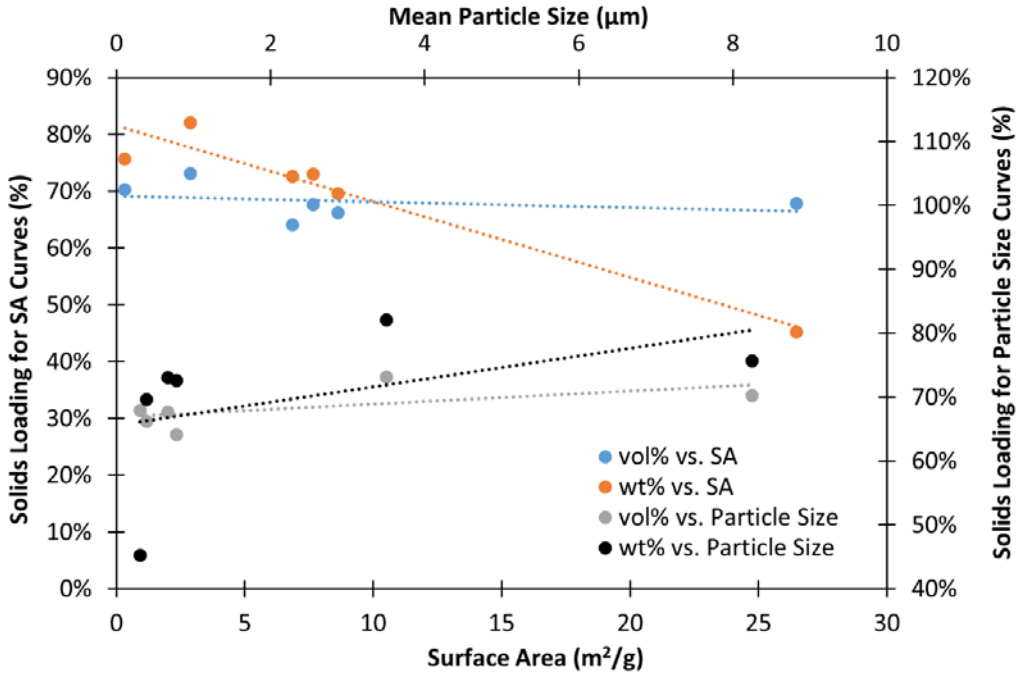

Fig. 8 Solids loading vs. particle size and surface area

4. Discussion

4.1 Determination of Gelation Time

The literature confirmed that gel time was a function of both the solids loading and binder content.[6,18] Keeping binder content constant and varying solids loading, a minimum gel time was achieved with a maximum solids loading. The lower solids loading required a longer time to gel due to the large gaps between particles. It also took more time for the particles to come together and for the binder coatings to interact. A higher solids loading would require less time simply because there is less space between the particles.

Additionally, there was a minimum observed in the binder content per solids added. This indicated that gel time trended with slurry viscosity and that the ideal binder content corresponded to approximately 0.3 solids wt%, the ideal minimum viscosity, in the case of alumina. A similar trend was often observed in slip casting slurries, where a dome type relationship occurred when viscosity was plotted against dispersant content. It was unknown whether the binder content would be consistent for other ceramics.

The gel time was observed to be volume dependent with larger castings taking more time to gel. It was for this reason that all of the gel time measurements were conducted on casts of approximately the same size. This indicated, in addition to a rapid gelling mechanism, that the setting mechanism was also controlled by water evaporation, which was similar to slip casting. Gelling created a semi-solid mass that could be inverted within the mold cavity, setting under capillary stress while the liquid was still evaporating, and causing the cast to contract slightly, consolidating it into a solid green body that could be demolded and transported. While the green bodies were only approximately 49% of theoretical density (TD), the air fired sintered bodies reach approximately 97% TD, indicating that sintering and particle rearrangement occurred as the polymer burned off. Full density could be reached with little difficulty by using an advanced sintering technique such as vacuum sintering to produce a driving force for pore collapse due to partial pressure gradients or hot isostatic pressing (HIP) to inhibit grain growth by allowing densification to occur more rapidly.

4.2 Mechanical Strength of Green Bodies

It was not expected that solids loading would have an effect on green body strength, since the polymer to ceramic ratio was kept constant at 0.3 wt% of the total solids. The increase may have been to the result of increased steric interactions between

ceramic particles due to proximity. In general, even when only mechanical pressure was used to densify green bodies, greater solids loading results in increased strength, as the particles deformed against each other. While no mechanical force was applied to the green bodies in this study, the decrease in inter-particle distance could also introduce some surface interactions due to proximity. The increase may have also indicated that the gelling mechanism is more similar to slip casting as opposed to traditional gel-casting. If gelling was the result of interaction of polymer chains between ceramic particles, as theorized, increasing the number of particles and thus decreasing the inter-particle distance would have allowed the same length polymer chain to interact with more of the ceramic surface (shorter bridging length). Increased interaction would lead to greater strength, as reflected in the data. More investigation is necessary to confirm this theory.

However, while trends were observed, only the pairs indicated in Tables 5 and 6 were found to be statistically different ($p<0.05$). The fact that not all pairs were found to be statistically different was likely due to the large variations observed. The variations were due to a lack of precision in the available load frame and load cell. A 1-kN load cell was used when forces observed were only on the order of 0.5-1 N, leading to issues with precise measurement. Additionally, a relatively low number of samples was tested. Current work in the Ceramics and Transparent Materials Branch within the US Army Research Laboratory is being done to improve upon these measurements and reduce the amount of variability in the data.

4.3 Slurry Behavior Trends with Surface Area and Particle Size

Six different alumina powders were gel-cast with a maximum amount of solids in the slurries. The goal was to observe a possible trend in particle size or surface area, with the batching recipe technique serving as a "trial and error" method. However, the only observed trend was that the weight percent solids loading decreased as the surface area increased. As the surface area increased, the powders became less dense and, in general, the decreased particle size saturated the slurries more quickly. However, the fact that the weight percent solids loading did not trend closely with particle size also indicated that the decrease in surface area was not due to particle size alone. Agglomerate size may have had more of an influence over the process than originally theorized. This was likely due to the binder interacting with agglomerates as opposed to primary particles. This observation made it even more critical to investigate how the binder would behave with fully dispersed suspensions that minimized the agglomerates. While the correlation coefficient was not statistically significant ($R^2 > 0.95$), it was still very high ($R^2 = 0.93$) for a data set

of only 6 points. More work will be done in this area to see if powder characteristics can be used to predict and engineer the desired gelling behavior, as these trends may apply to other ceramic systems.

For the powder samples with very large particle sizes (>1 μm), ISOBAM #110 (much higher molecular weight and thus longer chain length) had to be used to obtain the same gelling time. The observed viscosity remained approximately the same for all slurries with both ISOBAM chain lengths, but slurries composed of large primary particles took hours to set with the short chain ISOBAM (#104) versus 30–45 min for the long chain (#110). This is likely the result of surface adsorption, as polymer chains would adsorb onto the surface of the ceramic particles via hydrostatic interactions and hydrogen bonding while the ends would extend to bridge the gap between particles. The ends would then be free to interact with each other via the same weak bonding to stabilize the slurry into a gel over time. While more investigation into the mechanism will be conducted, it would be expected that as the particles get larger, longer chains would be required to have enough polymer chain to wrap around the particles while still being able to interact with each other enough to gel the slurry in a reasonable amount of time. More investigation is necessary.

5. Conclusion

These experiments were performed to learn how to control the ISOBAM system for ceramic processing, with a specific interest in optimizing the system for investigation of the applied magnetic field effects on micro-texture. As a result, effects of process variables such as slurry composition and particle size on set time and strength were of particular interest. Building upon current literature,[2–4,6,8–12,14] we have determined that gelling time changes with both solids loading and binder content, and confirmed that it also trends with viscosity. The fact that a minimum viscosity and minimum gel time were observed at an optimal binder content value (~0.3 solids wt%) indicated that the best way to modulate the gel time was to change the solids loading; as changing the binder content could have other adverse effects like prohibitively weak green bodies, incomplete dispersion (settling), or increased viscosity without increased solids loading. Furthermore, it was advantageous to maximize solids loading to minimize shrinkage and increase strength.

Shrinkage measurements exhibited typical behavior for gel-casting systems, as green bodies shrank approximately 50% throughout the processing sequence, but no cracking was observed. Complex-shaped pressureless sintered parts (Fig. 8) were easily cast with no cracking or warping. Pressureless sintered density measurements showed promising results for the potential use of the ISOBAM

gelling system for both general dense ceramic part production and transparent ceramic production, since more advanced techniques such as HIP or vacuum sintering could easily remove the final porosity. Additionally, the organic content was low to avoid potential second phase and inclusion contamination.

Attempts to construct a calibration curve showed that there was a correlation between surface area and solids loading in developing a successful slurry for casting. While more work was needed to confirm the behaviors observed and to investigate whether or not the trends apply to other ceramics systems, it was promising that gel casting formula parameters could be determined by calculations instead of trial and error, thus allowing this system to be applied to a wide range of powders and applications. Finally, several different complex shapes had been successfully cast into silicone candy molds, as shown in Fig. 9.

Fig. 9 Complex-shaped cast green body using the ISOBAM gelling system and slurry preparation procedure outlined in Section 2.2

6. References

1. Yang J, Yu J, Huang Y. Recent developments in gelcasting of ceramics. Journal of the European Ceramic Society. 2011;31(14):2569–2591.

2. Wan T, Yao D, Hu H, Xia Y, Zuo K, Zeng Y. Fabrication of porous Si_3N_4 ceramics through a novel gelcasting method. Materials Letters. 2014;133(15):190–192.

3. Sun Y, Shimai S, Peng X, Zhou G, Kamiya H, Wang S. Fabrication of transparent Y2O3 ceramics via aqueous gelcasting. Ceramics International. 2014;40(6):8841–8845.

4. Shu X, Li J, Zhang M, Dong M, Shunzo S. Gelcasting of aluminum nitride using a water-soluble copolymer. Journal of Inorganic Materials. 2014;29(3):327–330.

5. Wang Y, Zhou YJ, Cheng HF, Wang J. Gelcasting of sol-gel derived mullite based on gelation of modified poly (isobutylene-alt-maleic anhydride). Ceramics International. 2014;40(7):10565–10571.

6. Yang Y, Wu Y. New gelling systems to fabricate complex-shaped transparent ceramics. In: Tustison R, Zelinski B, editors. Proc. SPIE 8708, Window and Dome Technologies and Materials XIII; 2013 May 1–2; Baltimore, MD. Bellingham (WA): International Society for Optics and Photonics; c2013. p. 8708-44.

7. Suzuki TS, Sakka Y, Kitazawa K. Orientation amplification of alumina by colloidal filtration in a strong magnetic field and sintering. Advanced Engineering Materials. 2001;3(7):490–492.

8. Yang Y, Shimai S, Wang SW. Room-temperature gelcasting of alumina with a water-soluble copolymer. Journal of Materials Research. 2013;28(11):1512–1516.

9. Shimai S, Yang Y, Wang S, Kamiya H. Spontaneous gelcasting of translucent alumina ceramics. Opt Mater Express. 2013;3(8):1000–1006.

10. Sun Y, Shimai S, Peng X, Dong M, Kamiya H, Wang S. A method for gelcasting high-strength alumina ceramics with low shrinkage. Journal of Materials Research. 2014;29(2):247–251.

11. Yang Y, Wu YQ. Tape-casted transparent alumina ceramic wafers. Journal of Materials Research. 2014;29(19):2312–2317.

12. Deng XG, Wang J, Liu J, Zhang H, Li F, Duan H, Lu L, Huang Z, Zhao W, Zhang S. Preparation and characterization of porous mullite ceramics via foam-gelcasting. Ceramics International. 2015;41(7):9009–9017.

13. Wan T, Yao D, Hu H, Xia Y, Zuo K, Zeng Y. The microstructure and mechanical properties of porous silicon nitride ceramics prepared via novel aqueous gelcasting. International Journal of Applied Ceramic Technology. 2015;12(5):932–938.

14. Qin XP, Zhou G, Yang Y, Zhang J, Shu X, Shimai S, Wang S. Gelcasting of transparent YAG ceramics by a new gelling system. Ceramics International. 2014;40(8):12745–12750.

15. Wang J, Zhang F, Chen F, Zhang H, Tian R, Dong M, Liu J Zhang Z, Zhang J, Wang S. Fabrication of aluminum oxynitride (y-AlON) transparent ceramics with modified gelcasting. Journal of the American Ceramic Society. 2014;97(5):1353–1355.

16. Yang Y, Shimai S, Sun Y, Dong M, Kamiya H, Wang S. Fabrication of porous Al2O3 ceramics by rapid gelation and mechanical foaming. Journal of Materials Research. 2013;28(15):2012–2016.

17. Yang Y, Wei H, Zhang L, Kisslinger K, Melcher C, Wu Y. Blue emission of Eu2+-doped translucent alumina. Journal of Luminescence. 2015;168:297–303.

18. Yang Z, Yu J, Deng K, Lan L, Wang H, Ren Z, Wang Q, Dai Y, Wang H. Fabrication of textured Si3N4 ceramics with beta-Si3N4 powders as raw material by gel-casting under strong magnetic field. Materials Letters. 2014;135:218–221.

1 (PDF) DEFENSE TECHNICAL INFORMATION CTR DTIC OCA

2 (PDF) DIRECTOR US ARMY RESEARCH LAB RDRL CIO LL IMAL HRA MAIL & RECORDS MGMT

1 (PDF) GOVT PRINTG OFC A MALHOTRA

1 (PDF) DIR USARL RDRL WMM E V BLAIR